HHS Public Access

Author manuscript

Mol Cell. Author manuscript; available in PMC 2017 June 16.

Published in final edited form as:

Mol Cell. 2016 June 16; 62(6): 929–942. doi:10.1016/j.molcel.2016.04.023.

Inhibition of Rb phosphorylation leads to mTORC2-mediated activation of Akt

Jinfang Zhang[#2], **Kai Xu**[#1,2], **Pengda Liu**[2], **Yan Geng**[3], **Bin Wang**[2,4], **Wenjian Gan**[2], **Jianping Guo**[2], **Fei Wu**[2,6], **Y. Rebecca Chin**[2], **Christian Berrios**[5], **Evan C. Lien**[2], **Alex Toker**[2], **James A. DeCaprio**[5], **Piotr Sicinski**[3], and **Wenyi Wei**[2,7]

[1]Department of Otolaryngology-Head and Neck Surgery, Tongji Hospital, Tongji Medical College, Huazhong University of Science and Technology, Wuhan, 430030, P.R. China

[2]Department of Pathology, Beth Israel Deaconess Medical Center, Harvard Medical School, Boston, MA 02215, USA

[3]Department of Cancer Biology, Dana-Farber Cancer Institute and Department of Genetics, Harvard Medical School, Boston, MA 02115, USA

[4]Department of Gastroenterology, Institute of Surgery Research, Daping Hospital, Third Military Medical University, Chongqing, 400042, P. R. China

[5]Department of Medical Oncology, Dana-Farber Cancer Institute and Department of Medicine, Brigham and Women's Hospital, Harvard Medical School, Boston, MA 02215, USA

[6]Department of Urology, Huashan Hospital, Fudan University, Shanghai, 200040, P.R. China

[#] These authors contributed equally to this work.

SUMMARY

The retinoblastoma (Rb) protein exerts its tumor suppressor function primarily by inhibiting the E2F family of transcription factors that govern cell cycle progression. However, it remains largely elusive whether hyper-phosphorylated, non-E2F1-interacting form, of Rb has any physiological role. Here, we report that hyper-phosphorylated Rb directly binds to, and suppresses the function of mTORC2, but not mTORC1. Mechanistically, Rb, but not p107 nor p130, interacts with Sin1 and blocks the access of Akt to mTORC2, leading to attenuated Akt activation and increased sensitivity to chemotherapeutic drugs. As such, inhibition of Rb phosphorylation by depleting *cyclin D*, or using CDK4/6 inhibitors, releases Rb-mediated mTORC2 suppression. This, in turn, leads to elevated Akt activation to confer resistance to chemotherapeutic drugs in *Rb*-proficient

[7]To whom correspondence should be addressed: Wenyi Wei, Ph.D., Associate Professor, Department of Pathology, Beth Israel Deaconess Medical Center, Harvard Medical School, 3 Blackfan Circle, Boston, MA 02115, Phone: 617-735-2495; Fax: 617-735-2480, wwei2@bidmc.harvard.edu.

Author Contributions

J.Z., K.X., P.L. and W.W. designed experiments and wrote the manuscript. J.Z. and K.X. performed most of the experiments with help from P.L., Y.G., B.W., W.G., J.G., F.W., Y.C., C.B., E.L., A.T., and J.D.. W.W. and P.S. guided and supervised the project.

cells, which can be attenuated with Akt inhibitors. Therefore, our work provides a molecular basis for the synergistic usage of CDK4/6 and Akt inhibitors in treating *Rb*-proficient cancer.

Zhang *et al* report that hyper-phosphorylated Rb also plays a tumor suppressive role partly through binding Sin1 to inhibit mTORC2-mediated activation of Akt. Thus, inhibiting Rb phosphorylation by depletion of *cyclin D* or CDK4/6 inhibitor leads to elevated Akt-pS473 to confer drug resistance, which can be attenuated by Akt inhibitors.

Abstract

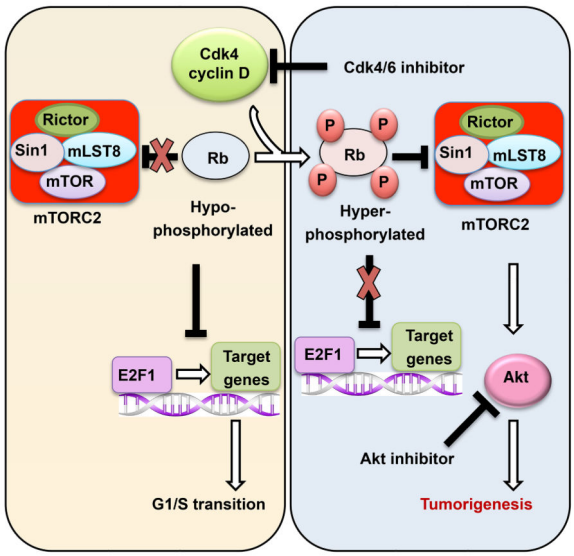

INTRODUCTION

Retinoblastoma (Rb) is a well-characterized tumor suppressor and its deregulation is frequently observed in various types of human cancers (Burkhart and Sage, 2008; Knudsen and Knudsen, 2008; Sherr and McCormick, 2002). Mechanistically, Rb exerts its tumor suppressor function primarily through direct binding and suppression of the E2F family of transcription factors in the nucleus, as well as governing $p27^{Kip1}$ stability in part through interacting with APC^{Cdh1} (Binne et al., 2007), leading to G1/S arrest during the cell cycle progression (van den Heuvel and Dyson, 2008). Notably, the transcriptional repressor activity of Rb can be antagonized by sequential phosphorylation events, initiated by cyclin D-CDK4/6 in the early G1 phase, followed by cyclin E-CDK2 in the late G1 phase (Knudsen and Knudsen, 2008). As a result, hyper-phosphorylated Rb loosens its association with chromatin (Mittnacht et al., 1994; Mittnacht and Weinberg, 1991) to release its suppressive role towards E2Fs in the nucleus. Notably, amplification or oncogenic mutations of Rb upstream negative regulators such as *cyclin D, CDK4, CDK6* or deletion of the CDK4/6 kinase inhibitor, $p16^{INK4a}$, are frequently observed in a majority of human cancer patients, which lead to hyper-phosphorylation of Rb, subsequently blocking interactions between Rb and E2Fs to inactivate the canonical tumor suppressor role of Rb (Burkhart and Sage, 2008; Choi et al., 2012).

In addition to the canonical function of Rb in regulating cell cycle progression in the nucleus, recent studies have also started to reveal a possible physiological role of Rb in the cytoplasm, such as regulating mitochondrial functions and disrupting sarcomeric organization (Araki et al., 2013; Hilgendorf et al., 2013; Nicolay et al., 2015). In support of these findings, the hyper-phosphorylated form of Rb has been observed in the cytoplasm of human cancers (Jiao et al., 2007). However, it remains largely undefined whether besides arresting the cell cycle by suppressing E2Fs, the non-E2F interacting hyper-phosphorylated Rb possesses any physiological function.

The human mTOR (mechanistic target of rapamycin) is a conserved multi-subunit serine/threonine kinase involved in governing a plethora of critical cellular processes including cell growth and proliferation (Wullschleger et al., 2006). Deregulation of the mTOR signaling pathway leads to various types of human diseases including human cancer (Cornu et al., 2013; Laplante and Sabatini, 2012; Xu et al., 2014; Zoncu et al., 2011). In cells, mTOR serves as an essential catalytic subunit by forming two structurally and functionally distinct complexes, mTORC1 and mTORC2, respectively. In addition to the common subunits including mTOR and GβL, Raptor defines mTORC1, whereas Rictor and Sin1 are specific components for the mTORC2 kinase complex (Laplante and Sabatini, 2012; Zoncu et al., 2011). Compared with the well-defined upstream signaling modulators of mTORC1 such as TSC1/2 (Inoki et al., 2002; Manning et al., 2002), PRAS40 (Sancak et al., 2007; Vander Haar et al., 2007), Rag (Kim et al., 2008; Sancak et al., 2008) and Rheb (Menon and Manning, 2013), the upstream signaling pathways governing the mTORC2 complex kinase activity remains largely elusive.

In this study, we report that hyper-phosphorylated Rb interacts with the mTORC2 complex to suppress Akt activation. Importantly, depletion of endogenous *cyclin D* or inhibition of CDK4/6 kinase activity by pharmacological inhibitors led to reduced Rb phosphorylation and attenuated Rb suppression on mTORC2 activation, resulting in elevated Akt phosphorylation and activation. Hence, our study provides a possible molecular mechanism for the synergistic usage of CDK4/6 and Akt inhibitors for better anti-cancer efficacy.

RESULTS

Rb negatively regulates the kinase activity of mTORC2, but not mTORC1, in cells

In searching for additional tumor suppressive mechanism(s) for Rb, we observed that in Cre-mediated *Rb*-deleted mouse embryonic fibroblasts ($Rb^{\Delta/\Delta}$ MEFs), Akt-pS473, the canonical substrate of mTORC2, was significantly elevated compared to control MEFs (*Rb*-WT MEFs) (Figure 1A). However, only a moderate elevation of Akt-pT308, and no significant change of S6K-pT389, indicators for activity of PDK1 and mTORC1, respectively, was observed between $Rb^{\Delta/\Delta}$ and *Rb*-WT MEFs (Figure 1A). Furthermore, genetic deletion of *Rb*, but not of Rb-related pocket proteins including *p107* or *p130*, led to increased Akt-pS473 (Figure S1A), demonstrating a unique role for Rb in suppressing mTORC2. In keeping with this finding, depletion of endogenous *Rb* in various tumor cell lines including OVCAR5 and MDA-MB-231 also led to a marked elevation in Akt-pS473, and to a much lesser extend, a moderate increase in Akt-pT308, but not S6K-pT389 (Figure 1B-C). As a

consequence, levels of Akt downstream targets pFOXO and PRAS40-pT246 were also dramatically increased in *Rb*-deficient cells (Figure 1A-C).

Given the well-characterized role of Rb in cell cycle regulation (van den Heuvel and Dyson, 2008) as well as the intrinsic connection between cell cycle and Akt activation (Liu et al., 2014), it is possible that the observed effects were caused by altered cell cycle progression of *Rb*-deficient cells. However, we observed no significant change of the cell cycle distribution profiles in $Rb^{-/-}$ MEFs, compared with WT counterparts (Figure S1B). Moreover, acutely induced expression of Rb led to a marked reduction of Akt-pS473 in cells (Figure 1D) without significantly affecting cell cycle (Figure S1C). Conversely, genetic ablation of *Rb*, resulted in sustained mTORC2 activation towards phosphorylating Akt-Ser473 upon stimulation by either insulin (Figure 1E and Figure S1D) or EGF (Figure 1F). On the other hand, ectopic expression of Rb attenuated Akt-pS473 upon EGF stimulation (Figure S1E) without significantly changing the cell cycle distribution (Figure S1F). Taken together, these results suggest that Rb largely inhibits the kinase activity of mTORC2, but not that of mTORC1 or PDK1 in cells.

Rb specifically interacts with the mTORC2 complex through binding the Sin1-PH domain

In order to identify whether Rb inhibits mTORC2 activity through binding its specific subunit, we examined the binding of Rb with all characterized mTOR complex subunits. Notably, we observed that Rb specifically interacted with the mTORC2-specifc component Sin1, but not Rictor, in Triton buffer that disrupts the complex integrity of both mTORC2 and mTORC1 (Kim et al., 2002) in U2OS cells (Figure 2A). Moreover, under the same experimental conditions, neither the mTORC1 specific subunit Raptor, nor the common mTOR complex subunits GβL or mTOR interacted with Rb (Figure 2A-B). Moreover, the interaction between Rb and Sin1 at endogenous levels was also observed in U2OS cells (Figure 2C). Interestingly, in 0.3% CHAPS containing buffer that preserves the integrity of mTOR complexes (Kim et al., 2002), Rb was able to precipitate the intact mTORC2 complex, but did not interact with the mTORC1 specific subunit, Raptor (Figure S2A). Furthermore, the endogenous binding of Rb with mTORC2 subunits, but not Raptor, was observed in multiple cell lines including U2OS (Figure 2D), OVCAR5 (Figure S2B) and MDA-MB-231 (Figure S2C). More importantly, we found that in $Sin1^{-/-}$ MEFs, Rb lost its ability to pull down any mTORC2 component, suggesting that Rb associates with mTORC2 in a Sin1-dependent manner (Figure 2E). These results establish the critical role of Sin1 in mediating the interaction of the mTORC2 complex with Rb.

Next, we found that Sin1 specifically interacted with Rb largely through the C-terminal PH domain in U2OS cells (Figure 2F-G). Moreover, bacterially purified GST-Sin1-PH, but not other domains, specifically pulled down Rb ectopically expressed in U2OS cells (Figure 2H), further supporting a specific interaction between Rb and the Sin1-PH domain. Notably, Rb interacted with the PH domain of Sin1, but not the PH domain of PDK1 or PLCD1 (Figure S2D-F), highlighting the specificity of Sin1-PH domain in recognizing Rb. Altogether, these data indicate that Rb might suppress Akt activity by directly interacting with the intact mTORC2 complexes, but not PDK1 or mTORC1, through binding the PH domain of Sin1. Hence, in the reminder study, we mainly focus on understanding

mechanistically how Rb suppresses Akt activity by interfering with mTORC2-mediated phosphorylation of Akt-S473.

Rb is a canonical pocket protein with three well-defined domains, including the amino-terminal domain (RBN), the central pocket domain, and the carboxyl-terminal domain (RBC) (van den Heuvel and Dyson, 2008) (Figure 2I). Interestingly, unlike canonical Rb-interacting proteins such as E2F1 that primarily binds the pocket domain of Rb (Burke et al., 2014; Rubin et al., 2005) (Figure 2J), Sin1 interacted with the RBC domain of Rb in cells (Figure 2K). This domain is poorly conserved between the three pocket proteins, explaining our observation that Sin1 interacted with Rb, but not the other two Rb-related pocket proteins, p107 and p130 (Classon and Harlow, 2002; Dick and Rubin, 2013) (Figure 2L). In keeping with this finding, endogenous Rb, but not other pocket proteins p107 and p130, were found to co-migrate with the intact mTORC2 complexes in U2OS cells (Figure S2G).

Rb interacts with Sin1 in an Rb-phosphorylation-dependent manner

As E2F1 and Sin1 bind to the pocket and RBC domains of Rb, respectively (Figure 2I-K), we next examined whether these two interactions were mediated through different molecular mechanisms. To this end, unlike the Rb/E2F1 interaction that occurs in the nucleus, Rb interacted with Sin1 mostly in the cytoplasm (Figure 3A). Moreover, a strong interaction between endogenous Rb and Sin1 was observed largely in the cytoplasm when using double thymidine to arrest U2OS cells at the G1/S boundary with enriched hyper-phosphorylated Rb species (Mittnacht et al., 1994; Mittnacht and Weinberg, 1991) (Figure 3B). Importantly, we further showed that dephosphorylation of Rb in cells by λ-phosphatase treatment, significantly reduced Rb interaction with Sin1 (Figure 3C), suggesting that the phosphorylated species of Rb favor Sin1 for interaction. In keeping with this notion, CDK4/6 inhibitor LEE011 treatment could dramatically decrease Rb interaction with Sin1 at endogenous levels in the cytoplasm (Figure 3D). To this end, at least 13 Ser/Thr residues in Rb have been previously shown to be phosphorylated by CDK4 and CDK2 during the late-G1/S cell cycle phase to dissociate E2F1 from Rb (Dick and Rubin, 2013) (Figure 3E). To further rigorously examine the role of Rb phosphorylation in mediating the interaction between Rb and Sin1, we utilized a Rb phospho-mimetic mutant (Rb-13E) and a phospho-deficient mutant (Rb-13A) (Barrientes et al., 2000; Dick and Rubin, 2013), respectively.

Importantly, compared with Rb-WT, the phospho-mimetic Rb-13E mutant displayed an enhanced interaction with endogenous Sin1, but an almost abolished binding to endogenous E2F1 that is consistent with a previous report (Lents et al., 2006) (Figure 3F and 3G). On the other hand, Rb-13A, the hypo-phospho-mimetic form of Rb prefered binding E2F1 to Sin1 (Figure 3F and 3G). Furthermore, bacterially purified Rb-13E, but not Rb-WT, efficiently suppressed active Sin1-containing mTORC2 kinase complexes towards phosphorylating Akt-Ser473 *in vitro* (Figure 3H). Together, these results highlight the importance of the phosphorylated forms of Rb in the direct suppression of mTORC2 kinase activity.

Furthermore, we examined whether Rb interaction with Sin1 is cell cycle-dependent. To this end, we synchronized U2OS cells at M phase by nocodazole treatment and released cells back into normal cycling conditions. Notably, we observed that Rb binding to Sin1 fluctuated during cell cycle with the strongest binding between Rb and Sin1 observed at 12

hours after nocodazole release, where most of cells were enriched at the late-G1 and S phases (Figure S3A-C). Moreover, although most of Rb was retained in the nucleus, a partial cytoplasmic localization of Rb was detected by immunofluorescence staining at 12 hours after nocodazole release (Figure S3D and S3E). Furthermore, cytoplasmic localization of phosphorylated Rb (Rb-pT821) was further confirmed by immunostaining in U2OS and OVCAR5 cells arrested at the G1/S phase by double thymidine treatment (Figure S3F). In keeping with a previous report (Jiao et al., 2006), increasing Rb phosphorylation through stable expression of a cyclin D/CDK4-R24C fusion protein (termed DK) (Binne et al., 2007) in human primary fibroblast cells also led to a partial Rb cytoplamic translocation (Figure S3G). Together, these results suggest that during the late-G1/S phase, hyper-phosphorylated Rb translocates into the cytoplasm and interacts with Sin1 to inhibit mTORC2 function.

Next, we examined the possible molecular mechanism(s) governing phospho-Rb-mediated suppression of the mTORC2 kinase activity. Notably, expression of either Rb-WT (Figure S3H) or Rb-13E (Figure S3I) did not affect the Sin1 binding to mTOR. These data indicated that Rb did not suppress mTORC2 by dissociating the integrity of the mTORC2 kinase complex. However, we observed that ectopically expressed Rb-WT (Figure 3I) and Rb-13E (Figure 3J), but not the Sin1 association-deficient Rb-13A (Figure 3K), competed with Akt1 as well as other Akt isoforms including Akt2 and Akt3 (Figure S3J and S3K) for binding to Sin1 in a dose-dependent manner. Furthermore, ectopic expression of Rb also partially blocked Sin1 interaction with SGK1, another well-characterized mTORC2 substrate (Lu et al., 2011; Pearce et al., 2011) in cells (Figure 3L). Cumulatively, these data indicate that the hyper-phosphorylated form of Rb may serve as an endogenous inhibitor for mTORC2 in part via blocking the substrates access to the mTORC2 kinase complex.

Interestingly, we found that loss of *PTEN* led to significantly reduced Rb interaction with Sin1 in cells (Figure 3M), presumably due to an elevated generation of $PI(3,4,5)P_3$ species (Song et al., 2012). We have recently reported that $PI(3,4,5)P_3$ binds the PH domain of Sin1 to release Sin1-PH domain mediated inhibition on mTORC2 (Liu et al., 2015). Given that both Rb and $PI(3,4,5)P_3$ bind the PH domain of Sin1, we next examined whether $PI(3,4,5)P_3$ competes with Rb in binding Sin1-PH domain. To this end, we found that $PI(3,4,5)P_3$ polysomes could attenuate Rb interaction with Sin1-PH domain (Figure S3L). However, Rb could not compete with $PI(3,4,5)P_3$ for interaction with the Sin1-PH domain (Figure S3M), nor release Sin1-PH domain binding with mTOR (Figure S3N). Furthermore, a Sin1-R393C/K428A/K464A mutant (termed as Sin1-CAA) deficient in binding $PI(3,4,5)P_3$ (Liu et al., 2015), exhibited an increased binding to Rb-WT and the Rb-13E mutant, compared to Sin1-WT (Figure S3O-P), further advocating for a dominant role of $PI(3,4,5)P_3$ in competing with Rb for binding the Sin1-PH domain. In keeping with this hypothesis, we found that ectopic expression of the two most common PI3KCA oncogenic mutants H1047R and E545K, could suppress Rb interaction with Sin1 at endogenous levels (Figure 3N and S3Q). Together, these data support the notion that $PI(3,4,5)P_3$ interaction with the Sin1-PH domain (Liu et al., 2015) may override Rb-mediated suppression of mTORC2.

Hyper-phosphorylated Rb inhibits mTORC2 kinase activity to suppress cell proliferation and sensitize cells to chemotherapeutic drugs

To examine the physiological role of phospho-Rb-mediated suppression of mTORC2 kinase activity in cells, we generated various cell lines stably expressing Rb-WT, Rb-13E or Rb-13A. Notably, in OVCAR5 cells, ectopic expression of the phospho-mimetic Rb-13E mutant led to a more dramatic reduction in Akt-pS473 than ectopic expression of Rb-WT at comparable levels, while expression of Rb-13A only minimally influenced Akt-pS473 (Figure 4A). Consistently, in $Rb^{-/-}$ MEFs, stable expression of Rb-13E led to a more dramatic reduction of Akt-pS473, compared with reintroducing Rb-WT or Rb-13A at comparable levels (Figure 4B), illustrating a critical role for the phosphorylated Rb species in actively suppressing the mTORC2/Akt signaling. In agreement with this finding, reconstitution of $Rb^{-/-}$ MEFs with Rb-13E led to a more dramatic reduction than ectopic expression of Rb-WT towards Akt activation upon insulin stimulation (Figure S4A-B), while on the other hand, expression of the Sin1 interaction-deficient form of Rb-13A in $Rb^{-/-}$ MEFs displayed a more sustained Akt activation (Figure S4A-B), consistent with its deficiency in inhibiting mTORC2 kinase activity. These results support the notion that under insulin stimulation condition, hyper-phosphorylated Rb is more potent towards inhibiting mTORC2 activation.

Notably, in keeping with previous reports (Herrera et al., 1996; Leng et al., 1997), flow cytometry analysis demonstrated that expression of either Rb-WT or Rb-13A in $Rb^{-/-}$ MEFs led to a significant arrest of cells in the G1 population, while expression of the non-E2F-interacting Rb-13E mutant did not exhibit a significant increase of G1 population compared to the EV-infected control cells (Figure S4C). Given that Akt activity is governed in a cell cycle-dependent manner and relatively enriched in the late S and G2/M phases (Liu et al., 2014), the observed G1 arrest by Rb-WT or Rb-13A might explain its moderate ability in reducing Akt-pS473 in $Rb^{-/-}$ MEFs (Figure 4B). On the other hand, Rb-13E displayed an enhanced capacity in suppressing Akt-pS473 (Figure 4B) without significantly changing cell cycle profile (Figure S4C), suggesting that Rb-13E may not suppress Akt activation through a secondary cell cycle effect. Interestingly, consistent with a more dramatic role of Rb-13A in suppressing cell cycle progression (Figure S4C) by an elevated interaction with E2Fs (Figure 3G), reintroducing Rb-13A led to the greatest reduction of cell proliferation than reintroducing Rb-WT or Rb-13E in $Rb^{-/-}$ MEFs (Figure 4C).

To further determine the physiological functions of hyper-phosphorylated Rb, we next examined whether phospho-Rb-mediated suppression of Akt activity affects cellular sensitivity to chemotherapeutic treatments. Given a critical role for Akt in pro-survival pathways and an elevated interaction between Rb-13E and Sin1 (Figure 3G) to suppress mTORC2 (Figure 4B), we observed that Rb-13E expressing $Rb^{-/-}$ MEFs were more sensitive to etoposide-induced cellular apoptosis than the cells expressing Rb-WT or Rb-13A (Figure 4D and 4F). Consistently, compared to Rb-13A or Rb-WT expressing cells, stably expressing Rb-13E in breast cancer cells MDA-MB-231 depleted of endogenous *Rb* also led to a marked induction of cellular apoptosis in response to etoposide (Figure 4E and 4G) or doxorubicin treatments (Figure S4D). Together, these results suggest that suppression

of the mTORC2/Akt pathway activation by hyper-phosphorylated Rb plays a critical role in regulating cellular sensitivity to chemotherapeutic agents.

Inhibition of Rb phosphorylation by *cyclin D* deficiency or CDK4/6 inhibitors leads to elevated Akt-pS473 to confer resistance to chemotherapeutic drugs

It has been well characterized that multi-site phosphorylation of Rb is initiated by CDK4/cyclin D (Halaban, 2005; Trimarchi and Lees, 2002). Consistent with a negative role of phospho-Rb in regulating Akt activation, we observed that genetic ablation of *cyclin D1* or *D2* led to a moderate increase of Akt-pS473, while deletion of *cyclin D3* resulted in significantly enhanced Akt-pS473 in primary MEFs (Figure 5A). Moreover, acutely depleting *cyclin D1* in OVCAR5 or MDA-MB-231 cells also resulted in an elevation of Akt-pS473 (Figure S5A and S5B). Strikingly, compared to WT MEFs, triple-knockout (TKO) MEFs lacking all three D-type cyclins (*cyclin D1*$^{-/-}$/*cyclin D2*$^{-/-}$/*cyclin D3*$^{-/-}$), displayed a significant elevation of Akt-pS473 (Figure 5B), in part due to reduced interaction between Rb and Sin1 in the cytoplasm of TKO MEFs (Figure S5C). As a consequence, compared with WT-MEFs, TKO MEFs exhibited a marked increase in cellular resistance to treatments with various chemotherapeutic drugs including etoposide (Figure 5C-D and Figure S5D-E), cisplatin (Figure 5E-F and Figure S5F-G) and doxorubicin (Figure S5H). Moreover, reintroduction of cyclin D1 into TKO MEFs led to increased Rb phosphorylation and a subsequent reduction in Akt-S473 phosphorylation (Figure S5I), which resulted in re-sensitization of TKO cells to etoposide (Figure 5G-H and S5J) or cisplatin (Figure 5I-J and S5K) treatment. Cumulatively, these data reveal that inhibition of Rb phosphorylation by genetic ablation of D-type cyclins, attenuates phosphor-Rb meditated suppression of mTORC2, which subsequently results in elevated Akt activity to confer chemotherapy resistance.

Given that the CDK4/6-cyclin D-Rb pathway has recently emerged as an attractive drug target for cancer therapies (Malumbres and Barbacid, 2009) and CDK4/6 inhibitors (including PD0332991, LEE011 and LY2835219) have shown promising clinical outcomes (Brower, 2014; Mayer, 2015), we next examined whether pharmacological inhibition of Rb phosphorylation by these CDK4/6 inhibitors would lead to elevated Akt activation. Indeed, we observed that all three CDK4/6 inhibitors including PD0332991, LEE011 and LY2835219, dramatically inhibited Rb phosphorylation and induced the phosphorylation of Akt-S473 in cells (Figure S5L). Furthermore, administration of PD0332991 led to an elevation of Akt-pS473 in *Rb*-WT, but not *Rb*-depleted OVCAR5 cells (Figure 5K), suggesting that treatment with PD0332991 results in elevated Akt activation largely in an Rb-dependent manner. Mechanistically, administration of PD0332991 caused reduced phosphorylation of Rb and correspondingly, attenuated Rb interaction with Sin1 in several cell lines including OVCAR5 (Figure 5L), U2OS (Figure S5M) and MDA-MB-231 (Figure S5N), thus releasing the blockage of access of Akt to mTORC2 mediated by Rb (Figure 3I-J) and leading to subsequent activation of Akt (Figure 5L). However, PD0332991 treatment did not significantly affect the interaction of Rb-13E mutant with Sin1 (Figure S5O). In keeping with this finding, in Rb-depleted MDA-MB-231 cells, administration of PD0332991 led to elevated Akt activation only in Rb-WT, but not in empty vector or Rb-13E expressing cells (Figure 5M). These findings indicate that treatment of cancer patients using CDK4/6

inhibitors would enhance Akt activation that may facilitate the development of drug resistance.

The synergistic usage of CDK4/6 and Akt inhibitors to treat human breast cancer with *Rb*-proficient genetic status

Previous studies showed that Rb is considered as a prognostic and interventional marker due to its genetic status determines sensitivity of tumors to chemotherapeutic drugs (Knudsen and Knudsen, 2008; Witkiewicz and Knudsen, 2014). Moreover, it was reported that combination of CDK4/6 and PI3K inhibitors could sensitize *PIK3CA* mutant breast cancer (Vora et al., 2014). However, the molecular mechanisms underlying the synergistic usage of CDK4/6 and PI3K inhibitors remain to be determined. Hence, our results indicate that CDK4/6 inhibitors could activate the Akt oncogenic signaling in part through releasing the phospho-Rb-mediated suppression of mTORC2 in *Rb*-proficient, but not in *Rb*-deficient cells. To test this model, we examined whether Akt inhibitors could synergistically function with CDK4/6 inhibitors to reduce cell viability and promote cell apoptosis in three *Rb*-proficient breast cancer cell lines (MDA-MB-453, MDA-MB-231 and Hs578T) and three *Rb*-deficient breast cancer cell lines (MDA-MB-436, MDA-MB-468 and BT549). The *Rb* status of these cell lines was confirmed (Figure S6A) as previously reported (Dean et al., 2012).

Notably, co-treatment with CDK4/6 and Akt inhibitors demonstrated a synergistic killing effect in *Rb*-proficient, but not in *Rb*-deficient breast cancer cells (Figure 6A-B), which was in large due to elevated cell apoptosis (Figure 6C-D). Mechanistically, treatments with CDK4/6 inhibitors alone significantly facilitated Akt activation in an Rb-dependent manner (Figure 6E-F), while co-treatment with CDK4/6 and Akt inhibitors led to the reduction of both phosporylation of Rb and Akt-S473 (Figure 6F), resulting in reduced cell viability and increased cell apoptosis. In keeping with this observation, stably expressing the constitutively active form of Akt (Myr-Akt) in *Rb*-proficient cells led to cellular resistance to the combinatory treatment (Figure 6G and S6B-C) largely through a robust induction of Akt-pS473 that is resistant to Akt inhibitor treatment. These results together reveal a physiological function of Rb in suppressing the mTORC2/Akt oncogenic signaling independent of its canonical role in suppressing E2F1-mediate cell cycle progression, and further suggest that the combinatorial usage of CDK4/6 and Akt inhibitors would achieve better treatment outcome in breast cancer patients with *Rb*-proficient genetic status.

DISCUSSION

During the G1/S transition, Rb is phosphorylated on multiple sites initiated by CDK4/cyclin D followed by action from the CDK2/cyclin E kinase (Mittnacht and Weinberg, 1991; Trimarchi and Lees, 2002), which loosens Rb interactions with chromatin to allow a subpopulation of phosphorylated Rb to translocate into the cytoplasm (Jiao et al., 2006; Russo et al., 2005). Historically, hyper-phosphorylated Rb has been generally considered as an inactive form of Rb due to the loss of its regulatory function in suppressing E2Fs-mediated transcription in the nucleus (Dick and Rubin, 2013). However, recent studies are beginning to reveal that the cytoplasmic Rb might also play important roles in regulating

mitochondrial functions and sarcomeric organization (Attardi and Sage, 2013; Hilgendorf et al., 2013; Nicolay et al., 2015). However, whether and how hyper-phosphorylated Rb exerts any physiological functions remains elusive.

In this study, we report that hyper-phosphorylated Rb functions as a negative regulator of the mTORC2 kinase complex, independent of its canonical, suppression of E2F-mediated transcriptional function by the hypo-phosphorylated form of Rb (Dick and Rubin, 2013). Specifically, we identified the unique mTORC2 component, Sin1, as a direct binding partner with the hyper-phosphorylated form of Rb. Furthermore, we showed that Rb mainly used the C-terminal RBC domain to associate with the Sin1-PH motif to efficiently block the access of mTORC2 substrates to mTORC2 for subsequent phosphorylation and activation. Thus, the physiological function of Rb consists of two independent circuits (Figure S6D): hypo-phosphorylated Rb mainly binds and suppresses E2F1 to arrest cell cycle at G1 phase, while the hyper-phosphorylated species of Rb become loosely interacted with chromatin and partly translocates into the cytoplasm to bind and inhibit mTORC2 towards activating the Akt oncogenic signaling pathways. However, as Rb can impact mitochondrial biogenesis and function in cytoplasm (Araki et al., 2013; Attardi and Sage, 2013; Hilgendorf et al., 2013; Nicolay et al., 2015), future study is warranted to explore whether hyper-phosphorylated Rb also can indirectly affect mTORC2 through regulating mitochondrial functions.

The sequential phosphorylation of Rb by CDK4/6-cyclin D and CDK2-cyclin E is critical for releasing E2Fs and cell-cycle entry (Trimarchi and Lees, 2002). However, mice lacking individual D-type cyclins are viable and display minor phenotypes (Fantl et al., 1995; Sicinska et al., 2003; Sicinski et al., 1996). In addition, mice lacking all three D-type cyclins (*cyclin D1*$^{-/-}$*D2*$^{-/-}$*D3*$^{-/-}$ mice) develop relatively normally until mid-gestation, in part due to compensatory effects of the E-type cyclins (Geng et al., 2003; Kozar et al., 2004). Our results reveal that genetic ablation of all D-type cyclins leads to elevated Akt-pS473 (Figure 5B), which could protect cells from apoptosis and might explain one of the compensatory mechanisms of cell survival in *cyclin D1*$^{-/-}$*D2*$^{-/-}$*D3*$^{-/-}$ mice.

The majority of human cancers have mutually exclusive active mutations of *cyclin D* or *CDK4/6*, or inactive mutation of *p16*^{INK4a}, all of which will lead to phosphorylation of Rb (Trimarchi and Lees, 2002). Our results indicate that suppression of Rb phosphorylation through inhibition of CDK4/6 activity by its pharmacological inhibitors or by depletion of its substrate-binding partner *cyclin D*, led to elevated mTORC2 activity to confer chemotherapy resistance (Figure 5). As such, combination of CDK4/6 and Akt inhibitors could synergistically reduce cell viability and increase cell apoptosis in *Rb*-proficient breast cancer cells (Figure 6). Hence, our study provides the molecular insights into an E2Fs-independent, physiological role of Rb in suppressing the mTORC2/Akt oncogenic pathway in part by governing the substrate access to mTORC2, and further suggests that it is beneficial to clinically combine the CDK4/6 and Akt inhibitors to treat human cancers with *Rb*-proficient genetic status.

Experimental Procedures

Immunoblot and immunoprecipitation

Cells were lysed in Triton lysis buffer (50 mM Tris pH 7.5, 120 mM NaCl, 1% Triton), EBC buffer (50 mM Tris pH 7.5, 120 mM NaCl, 0.5% NP40) or 0.3% CHAPS lysis buffer (50 mM Tris pH 7.5, 120 mM NaCl, 1mM EDTA, 0.3% CHAPS) supplemented with protease inhibitors (Roche) and phosphatase inhibitors (Calbiochem). The protein concentrations of lysates were measured by Beckman Coulter DU-800 spectrophotometer using the Bio-Rad protein assay reagent. For immunoprecipitation assays, 1000 μg lysates were incubated with the appropriate antibody-conjugatd beads (1-2 μg) for 4 hours or overnight at 4°C. The total cell lysates and immunocomplexes were resolved by SDS-PAGE and immunoblotted with indicated antibodies.

In vitro kinase assays

In vitro kinase assay was conducted following previous protocol (Liu et al., 2013). Briefly, increasing doses (0, 0.5 μg and 1 μg) of bacterially purified His-tag Rb protein were incubated with HA-Sin1 immunoprecipitated active mTORC2 complex products from 4 mg of whole cell lysates ectopically expressing HA-Sin1, in the presence of 1 μg GST-Akt-tail (408-480) fusion protein, 0.1 mM ATP and kinase reaction buffer (10 μM Tris-HCl, pH7.5, 10 mM $MgCl_2$, 0.1 mM EDTA and 2 mM DTT) at 30°C for 30 min. The reaction was stopped by the addition of SDS-containing lysis buffer and resolved by SDS-PAGE. Phosphorylation of GST-Akt1-tail was detected by immunoblot with anti-phospho-Ser473-Akt antibody.

Annexin-V/7-AAD double staining

For detection of apoptosis, cells treated with indicated concentration of etoposide (Sigma, E1383) or cisplatin (Selleck, S1166) were co-stained with Annexin-V-PE and 7-AAD (Annexin V-PE Apoptosis Detection Kit I, BD Bioscience) according to the manufacturer's instructions. Stained cells were sorted with FACS.

Cell viability assays

For cell viability assays, 3000 per well cells were plated in 96-well plates, and incubated with complete DMEM medium containing different concentrations of etoposide (Sigma, E1383), cisplatin (Selleck, S1166) or doxorubicin (Sigma, D1515) for 24 h or 48 h. Assays were performed with the Cell Titer-Glo Luminescent Cell Viability Assay Kit according to the manufacturer's instructions (Promega). *Cyclin* $D1^{-/-}$ $D2^{-/-}D3^{-/-}$ MEFs were derived from E13.5 mouse embryos and immortalized with dominant-negative p53 as described before (Kozar et al., 2004).

Statistical analyses

All quantitative data were presented as the mean ± sd as indicated of at least three independent experiments by Student's *t* test between group differences. * $p < 0.05$ indicates significant.

Supplementary Material

Refer to Web version on PubMed Central for supplementary material.

Acknowledgments

We thank B. North, H. Inuzuka, X. Dai and other Wei lab members for critical reading of the manuscript, Julien Sage, David Goodrich and Nicolas Dyson for providing valuable reagents. W.W. is an ACS scholar. P.L. is supported by 1K99CA181342. J.G. is an NRSA T32 trainee and supported by 5T32HL007893-17. This work was supported in part by the NIH grants (R01CA177910 and R01GM094777 to W.W.; R01CA083688 and R01CA132740-08 to P.S.).

REFERENCES

Araki K, Kawauchi K, Hirata H, Yamamoto M, Taya Y. Cytoplasmic translocation of the retinoblastoma protein disrupts sarcomeric organization. Elife. 2013; 2:e01228. [PubMed: 24302570]

Attardi LD, Sage J. RB goes mitochondrial. Genes Dev. 2013; 27:975–979. [PubMed: 23651852]

Barrientes S, Cooke C, Goodrich DW. Glutamic acid mutagenesis of retinoblastoma protein phosphorylation sites has diverse effects on function. Oncogene. 2000; 19:562–570. [PubMed: 10698526]

Binne UK, Classon MK, Dick FA, Wei W, Rape M, Kaelin WG Jr. Naar AM, Dyson NJ. Retinoblastoma protein and anaphase-promoting complex physically interact and functionally cooperate during cell-cycle exit. Nat Cell Biol. 2007; 9:225–232. [PubMed: 17187060]

Brower V. Cell cycle inhibitors make progress. J Natl Cancer Inst. 2014; 106:2–4.

Burke JR, Liban TJ, Restrepo T, Lee HW, Rubin SM. Multiple mechanisms for E2F binding inhibition by phosphorylation of the retinoblastoma protein C-terminal domain. J Mol Biol. 2014; 426:245–255. [PubMed: 24103329]

Burkhart DL, Sage J. Cellular mechanisms of tumour suppression by the retinoblastoma gene. Nat Rev Cancer. 2008; 8:671–682. [PubMed: 18650841]

Choi YJ, Li X, Hydbring P, Sanda T, Stefano J, Christie AL, Signoretti S, Look AT, Kung AL, von Boehmer H, et al. The requirement for cyclin D function in tumor maintenance. Cancer Cell. 2012; 22:438–451. [PubMed: 23079655]

Classon M, Harlow E. The retinoblastoma tumour suppressor in development and cancer. Nat Rev Cancer. 2002; 2:910–917. [PubMed: 12459729]

Cornu M, Albert V, Hall MN. mTOR in aging, metabolism, and cancer. Curr Opin Genet Dev. 2013; 23:53–62. [PubMed: 23317514]

Dean JL, McClendon AK, Knudsen ES. Modification of the DNA damage response by therapeutic CDK4/6 inhibition. J Biol Chem. 2012; 287:29075–29087. [PubMed: 22733811]

Dick FA, Rubin SM. Molecular mechanisms underlying RB protein function. Nat Rev Mol Cell Biol. 2013; 14:297–306. [PubMed: 23594950]

Fantl V, Stamp G, Andrews A, Rosewell I, Dickson C. Mice lacking cyclin D1 are small and show defects in eye and mammary gland development. Genes Dev. 1995; 9:2364–2372. [PubMed: 7557388]

Geng Y, Yu Q, Sicinska E, Das M, Schneider JE, Bhattacharya S, Rideout WM, Bronson RT, Gardner H, Sicinski P. Cyclin E ablation in the mouse. Cell. 2003; 114:431–443. [PubMed: 12941272]

Halaban R. Rb/E2F: a two-edged sword in the melanocytic system. Cancer Metastasis Rev. 2005; 24:339–356. [PubMed: 15986142]

Herrera RE, Sah VP, Williams BO, Makela TP, Weinberg RA, Jacks T. Altered cell cycle kinetics, gene expression, and G1 restriction point regulation in Rb-deficient fibroblasts. Mol Cell Biol. 1996; 16:2402–2407. [PubMed: 8628308]

Hilgendorf KI, Leshchiner ES, Nedelcu S, Maynard MA, Calo E, Ianari A, Walensky LD, Lees JA. The retinoblastoma protein induces apoptosis directly at the mitochondria. Genes Dev. 2013; 27:1003–15. [PubMed: 23618872]

Inoki K, Li Y, Zhu T, Wu J, Guan KL. TSC2 is phosphorylated and inhibited by Akt and suppresses mTOR signalling. Nat cell biol. 2002; 4:648–657. [PubMed: 12172553]

Jiao W, Datta J, Lin HM, Dundr M, Rane SG. Nucleocytoplasmic Shuttling of the Retinoblastoma Tumor Suppressor Protein via Cdk Phosphorylation-dependent Nuclear Export. J Biol Chem. 2006; 281:38098–108. [PubMed: 17043357]

Jiao W, Lin HM, Datta J, Braunschweig T, Chung J-Y, Hewitt SM, Rane SG. Aberrant nucleocytoplasmic localization of the retinoblastoma tumor suppressor protein in human cancer correlates with moderate/poor tumor differentiation. Oncogene. 2007; 27:3156–64. [PubMed: 18071317]

Kim DH, Sarbassov DD, Ali SM, King JE, Latek RR, Erdjument-Bromage H, Tempst P, Sabatini DM. mTOR interacts with raptor to form a nutrient-sensitive complex that signals to the cell growth machinery. Cell. 2002; 110:163–175. [PubMed: 12150925]

Kim E, Goraksha-Hicks P, Li L, Neufeld TP, Guan KL. Regulation of TORC1 by Rag GTPases in nutrient response. Nat Cell Biol. 2008; 10:935–945. [PubMed: 18604198]

Knudsen ES, Knudsen KE. Tailoring to RB: tumour suppressor status and therapeutic response. Nat Rev Cancer. 2008; 8:714–724. [PubMed: 19143056]

Kozar K, Ciemerych MA, Rebel VI, Shigematsu H, Zagozdzon A, Sicinska E, Geng Y, Yu Q, Bhattacharya S, Bronson RT, et al. Mouse development and cell proliferation in the absence of D-cyclins. Cell. 2004; 118:477–491. [PubMed: 15315760]

Laplante M, Sabatini DM. mTOR signaling in growth control and disease. Cell. 2012; 149:274–293. [PubMed: 22500797]

Leng X, Connell-Crowley L, Goodrich D, Harper JW. S-Phase entry upon ectopic expression of G1 cyclin-dependent kinases in the absence of retinoblastoma protein phosphorylation. Curr Biol. 1997; 7:709–712. [PubMed: 9285720]

Lents NH, Gorges LL, Baldassare JJ. Reverse mutational analysis reveals threonine-373 as a potentially sufficient phosphorylation site for inactivation of the retinoblastoma tumor suppressor protein (pRB). Cell Cycle. 2006; 5:1699–1707. [PubMed: 16880741]

Liu P, Begley M, Michowski W, Inuzuka H, Ginzberg M, Gao D, Tsou P, Gan W, Papa A, Kim BM, et al. Cell-cycle-regulated activation of Akt kinase by phosphorylation at its carboxyl terminus. Nature. 2014; 508:541–545. [PubMed: 24670654]

Liu P, Gan W, Chin YR, Ogura K, Guo J, Zhang J, Wang B, Blenis J, Cantley LC, Toker A, et al. PtdIns(3,4,5)P3-Dependent Activation of the mTORC2 Kinase Complex. Cancer discovery. 2015; 5:1194–1209. [PubMed: 26293922]

Liu P, Gan W, Inuzuka H, Lazorchak AS, Gao D, Arojo O, Liu D, Wan L, Zhai B, Yu Y, et al. Sin1 phosphorylation impairs mTORC2 complex integrity and inhibits downstream Akt signalling to suppress tumorigenesis. Nat Cell Biol. 2013; 15:1340–1350. [PubMed: 24161930]

Lu M, Wang J, Ives HE, Pearce D. mSIN1 protein mediates SGK1 protein interaction with mTORC2 protein complex and is required for selective activation of the epithelial sodium channel. J Biol Chem. 2011; 286:30647–30654. [PubMed: 21757730]

Malumbres M, Barbacid M. Cell cycle, CDKs and cancer: a changing paradigm. Nat Rev Cancer. 2009; 9:153–166. [PubMed: 19238148]

Manning BD, Tee AR, Logsdon MN, Blenis J, Cantley LC. Identification of the tuberous sclerosis complex-2 tumor suppressor gene product tuberin as a target of the phosphoinositide 3-kinase/akt pathway. Mol Cell. 2002; 10:151–162. [PubMed: 12150915]

Mayer EL. Targeting Breast Cancer with CDK Inhibitors. Curr Oncol Rep. 2015; 17:443. [PubMed: 25716100]

Menon S, Manning BD. Cell signalling: nutrient sensing lost in cancer. Nature. 2013; 498:444–445. [PubMed: 23803840]

Mittnacht S, Lees JA, Desai D, Harlow E, Morgan DO, Weinberg RA. Distinct sub-populations of the retinoblastoma protein show a distinct pattern of phosphorylation. EMBO J. 1994; 13:118–127. [PubMed: 8306955]

Mittnacht S, Weinberg RA. G1/S phosphorylation of the retinoblastoma protein is associated with an altered affinity for the nuclear compartment. Cell. 1991; 65:381–393. [PubMed: 2018973]

Nicolay BN, Danielian PS, Kottakis F, Lapek JD Jr. Sanidas I, Miles WO, Dehnad M, Tschop K, Gierut JJ, Manning AL, et al. Proteomic analysis of pRb loss highlights a signature of decreased mitochondrial oxidative phosphorylation. Genes Dev. 2015; 29:1875–1889. [PubMed: 26314710]

Pearce LR, Sommer EM, Sakamoto K, Wullschleger S, Alessi DR. Protor-1 is required for efficient mTORC2-mediated activation of SGK1 in the kidney. Biochem J. 2011; 436:169–179. [PubMed: 21413931]

Rubin SM, Gall AL, Zheng N, Pavletich NP. Structure of the Rb C-terminal domain bound to E2F1-DP1: a mechanism for phosphorylation-induced E2F release. Cell. 2005; 123:1093–1106. [PubMed: 16360038]

Russo G, Zamparelli A, Howard CM, Minimo C, Bellan C, Carillo G, Califano L, Leoncini L, Giordano A, Claudio PP. Expression of cell cycle-regulated proteins pRB2/p130, p107, E2F4, p27, and pCNA in salivary gland tumors: prognostic and diagnostic implications. Clin Cancer Res. 2005; 11:3265–3273. [PubMed: 15867222]

Sancak Y, Peterson TR, Shaul YD, Lindquist RA, Thoreen CC, Bar-Peled L, Sabatini DM. The Rag GTPases bind raptor and mediate amino acid signaling to mTORC1. Science. 2008; 320:1496–1501. [PubMed: 18497260]

Sancak Y, Thoreen CC, Peterson TR, Lindquist RA, Kang SA, Spooner E, Carr SA, Sabatini DM. PRAS40 is an insulin-regulated inhibitor of the mTORC1 protein kinase. Mol Cell. 2007; 25:903–915. [PubMed: 17386266]

Sherr CJ, McCormick F. The RB and p53 pathways in cancer. Cancer Cell. 2002; 2:103–112. [PubMed: 12204530]

Sicinska E, Aifantis I, Le Cam L, Swat W, Borowski C, Yu Q, Ferrando AA, Levin SD, Geng Y, von Boehmer H, et al. Requirement for cyclin D3 in lymphocyte development and T cell leukemias. Cancer Cell. 2003; 4:451–461. [PubMed: 14706337]

Sicinski P, Donaher JL, Geng Y, Parker SB, Gardner H, Park MY, Robker RL, Richards JS, McGinnis LK, Biggers JD, et al. Cyclin D2 is an FSH-responsive gene involved in gonadal cell proliferation and oncogenesis. Nature. 1996; 384:470–474. [PubMed: 8945475]

Song MS, Salmena L, Pandolfi PP. The functions and regulation of the PTEN tumour suppressor. Nat Rev Mol Cell Biol. 2012; 13:283–296. [PubMed: 22473468]

Trimarchi JM, Lees JA. Sibling rivalry in the E2F family. Nat Rev Mol Cell Biol. 2002; 3:11–20. [PubMed: 11823794]

van den Heuvel S, Dyson NJ. Conserved functions of the pRB and E2F families. Nat Rev Mol Cell Biol. 2008; 9:713–724. [PubMed: 18719710]

Vander Haar E, Lee SI, Bandhakavi S, Griffin TJ, Kim DH. Insulin signalling to mTOR mediated by the Akt/PKB substrate PRAS40. Nat Cell Biol. 2007; 9:316–323. [PubMed: 17277771]

Vora SR, Juric D, Kim N, Mino-Kenudson M, Huynh T, Costa C, Lockerman EL, Pollack SF, Liu M, Li X, et al. CDK 4/6 inhibitors sensitize PIK3CA mutant breast cancer to PI3K inhibitors. Cancer cell. 2014; 26:136–149. [PubMed: 25002028]

Witkiewicz AK, Knudsen ES. Retinoblastoma tumor suppressor pathway in breast cancer: prognosis, precision medicine, and therapeutic interventions. Breast Cancer Res. 2014; 16:207. [PubMed: 25223380]

Wullschleger S, Loewith R, Hall MN. TOR signaling in growth and metabolism. Cell. 2006; 124:471–484. [PubMed: 16469695]

Xu K, Liu P, Wei W. mTOR signaling in tumorigenesis. Biochim Biophys Acta. 2014; 1846:638–654. [PubMed: 25450580]

Zoncu R, Efeyan A, Sabatini DM. mTOR: from growth signal integration to cancer, diabetes and ageing. Nat Rev Mol Cell Biol. 2011; 12:21–35. [PubMed: 21157483]

Highlights

- Rb, but not p107 nor p130, negatively regulates the kinase activity of mTORC2
- Hyper-phosphorylated Rb interacts with Sin1 to block the access of Akt to mTORC2
- Inhibiting Rb phosphorylation leads to elevated Akt-pS473 to confer drug resistance
- CDK4/6 inhibitor synergizes with Akt inhibitor in treating Rb-positive cancer cells

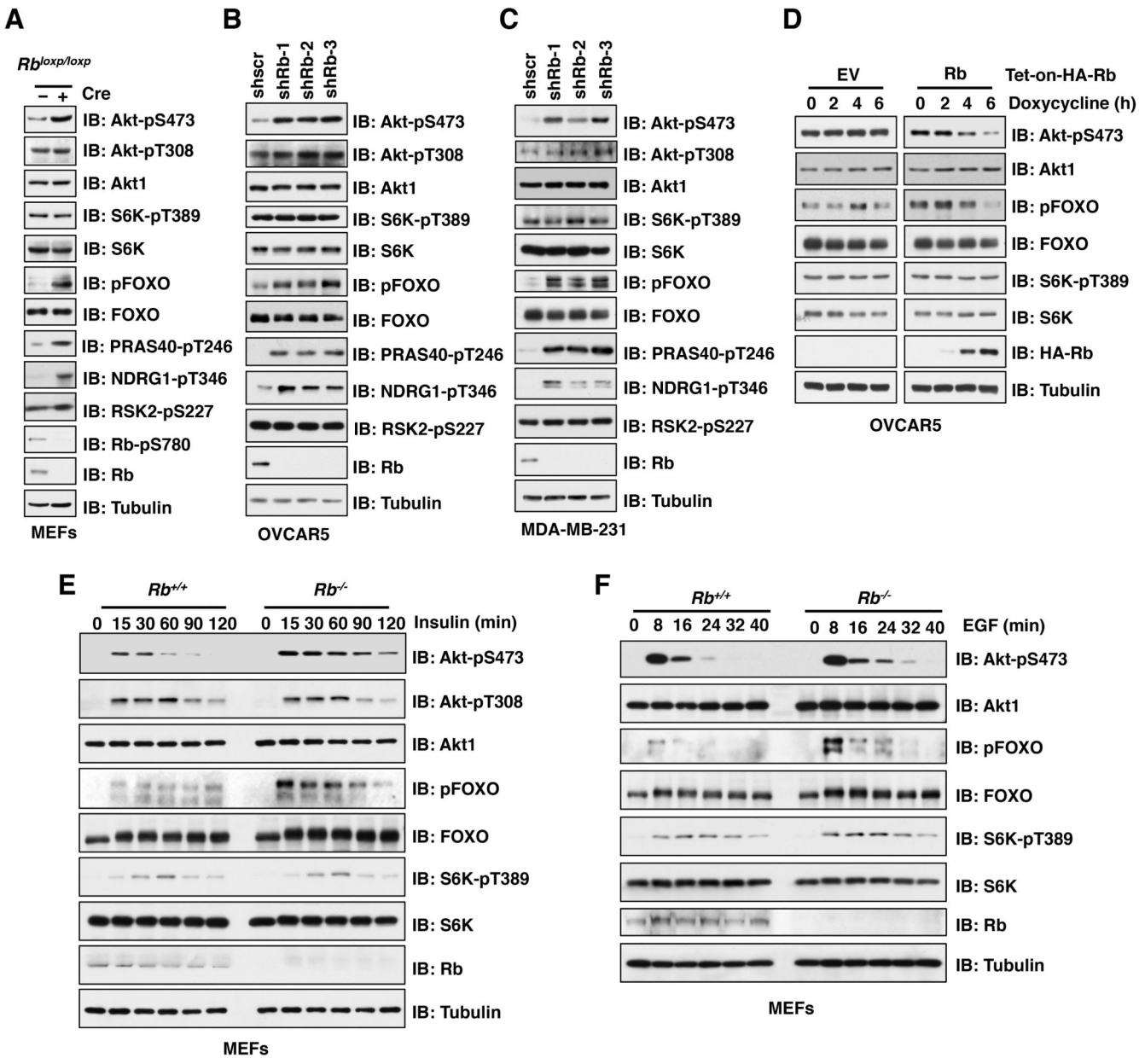

Figure 1. Rb negatively regulates the mTORC2, but not mTORC1 activity

A. Immunoblot (IB) analysis of whole cell lysates (WCL) derived from *Rb*$^{loxp/loxp}$ MEFs depleted Rb by pBabe-Cre via viral infection (pBabe-EGFP as a negative control), selected with puromycin (1 μg/ml) for more than 3 days.

B and C. IB analysis of WCL derived from OVCAR5 (**B**) and MDA-MB-231 (**C**) cells depleted of *Rb* by three independent shRNAs (shScramble as a negative control).

D. IB analysis of WCL derived from OVCAR5 cells stably expressing inducible pTRIPZ-YFP and pTRIPZ-HA-Rb treated with doxycycline (500 ng/ml) for the indicated periods.

E and F. *Rb*$^{+/+}$ and *Rb*$^{-/-}$ MEFs were serum starved for 36 h before harvesting for IB analysis after treatment with insulin (0.1 μM) (**E**) or EGF (100 ng) (**F**) with indicated time periods.

(See also Figure S1)

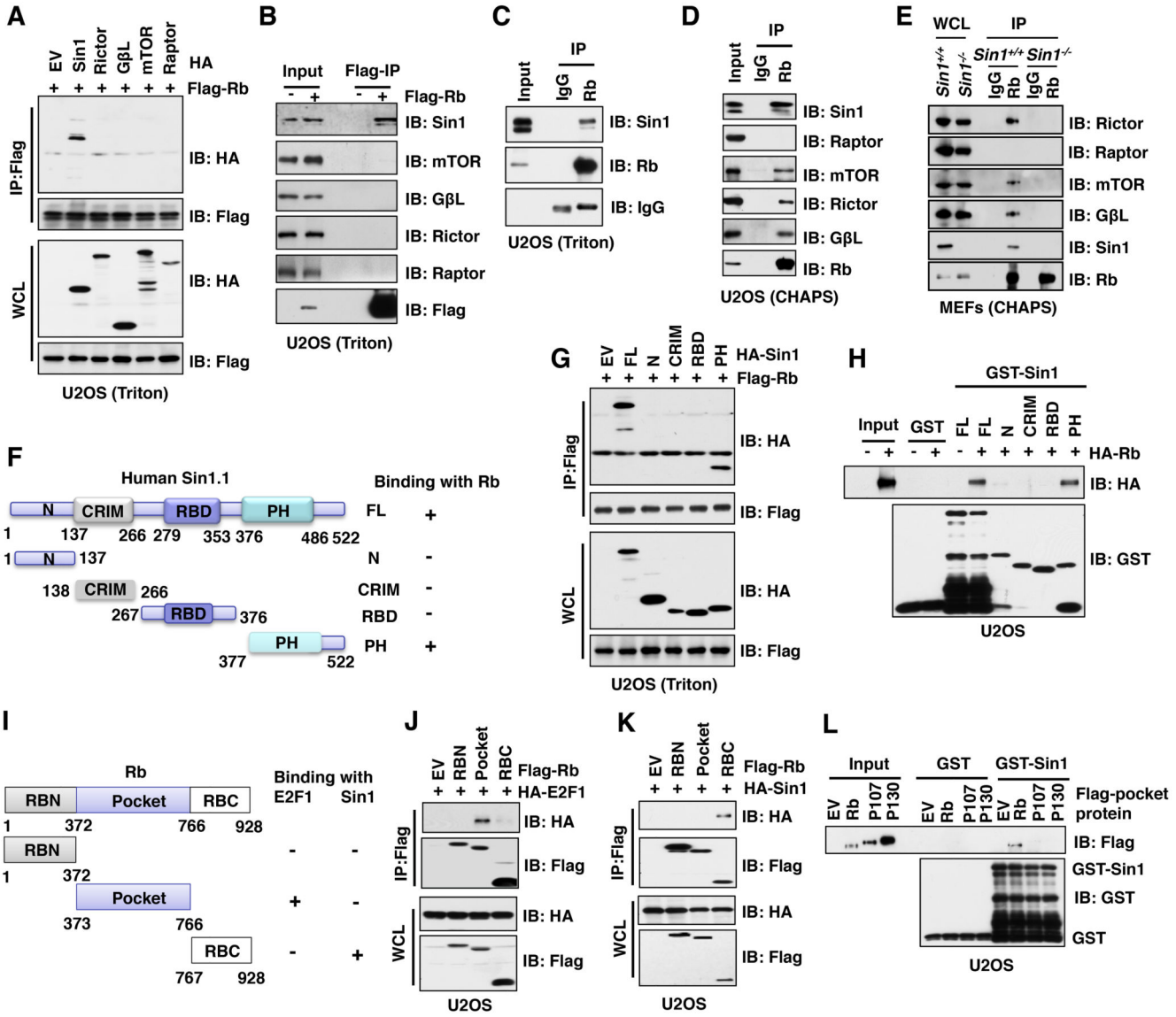

Figure 2. Rb interacts with the intact mTORC2 kinase complex through directly binding the Sin1-PH domain

A. IB analysis of WCL and anti-Flag immunoprecipitates (IP) derived from U2OS cells lysed in 1% Triton buffer 36 h after transfected with Flag-Rb and a whole panel of various indicated mTORC component subunits.

B. IB analysis of WCL and Flag-IP derived from U2OS cells lysed in 1% Triton buffer 36 h after transfected with empty vector and Flag-Rb.

C. IB analysis of WCL and endogenous Rb-IP derived from U2OS cells lysed in 1% Triton buffer.

D. IB analysis of WCL and endogenous Rb-IP derived from U2OS cells lysed in 0.3% CHAPS buffer.

E. IB analysis of WCL and endogenous Rb-IP derived from *Sin1*$^{+/+}$ MEFs and *Sin1*$^{-/-}$ MEFs lysed in 0.3% CHAPS buffer.

F. A schematic representation of the indicated domains of Sin1 and a summary of the Rb interacting ability of each domain within Sin1.
G. IB analysis of WCL and HA-IP derived from U2OS cells lysed in 1% Triton buffer 36 h after transfected Flag-Rb together with indicated HA-Sin1 truncating constructs.
H. GST pull-down assays to demonstrate that the Sin1-PH domain associates with Rb.
I. A schematic representation of the indicated region of Rb used in this study.
J. IB analysis of anti-Flag IP and WCL derived from U2OS cells lysed in 1% Triton buffer 36 h after transfection with indicated constructs
K. IB analysis of WCL and anti-Flag IP derived from U2OS cells lysed in 1% Triton buffer 36 h after transfection with HA-Sin1 and a whole panel of the indicated Rb truncation constructs.
L. GST pull-down assays to demonstrate that Sin1 directly interacts with Rb, but not other pocket proteins we examined.
(See also Figure S2)

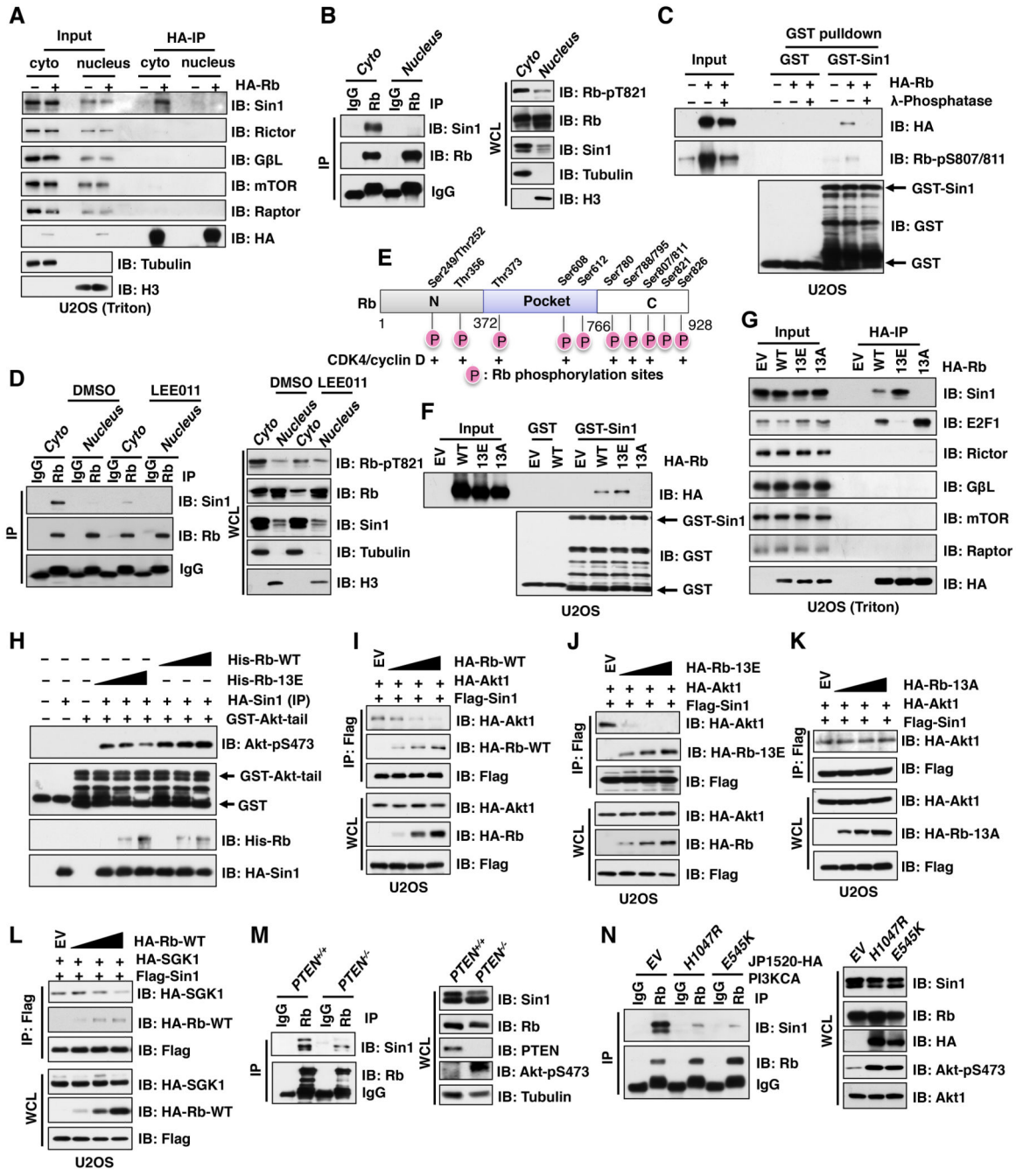

Figure 3. Rb interacts with Sin1 in a Rb phosphorylation-dependent manner

A. IB analysis of anti-HA IP and WCL derived from equal amounts of cytoplasmic lysate versus nuclear lysate in 1% Triton buffer. Histone-H3 and Tubulin were used as a nucleic fraction and cytoplasmic marker, respectively.

B. IB analysis of anti-Rb IP and WCL derived from equal amounts of cytoplasmic and nuclear lysate. Before harvesting for cytoplasm/nuclear fractionation, U2OS cells were arrested at the G1/S boundary by the double thymidine block method.

C. IB analysis of WCL and GST pull-down assay derived from U2OS cells lysed in 1% Triton buffer 36 h after transfection with HA-Rb. The lysates were treated with λ-phosphatase for 30 min in 30°C.

D. IB analysis of anti-Rb IP and WCL derived from equal cytoplasmic and nucleic fraction. Before harvesting for cytoplasm/nuclear fractionation, U2OS cells were treated with the CDK4/6 inhibitor, LEE011 (1 μM), for 24 h.

E. A schematic representation of the indicated phosphorylation sites of Rb. The 13 major CDK4/cyclin D phosphorylation sites on Rb were changed into alanines (13A) or glutamic acid (13E) for following up studies.

F. IB analysis of WCL and GST pull-down derived from U2OS cells lysed in 1% Triton buffer 36 h after transfection with indicated HA-Rb constructs.

G. IB analysis of WCL and anti-HA IP derived from U2OS cells lysed in 1% Triton buffer 36 h after transfection with empty vector and indicated HA-Rb constructs.

H. HEK293 cells were transfected with the HA-Sin1. Cells were serum-starved for 12 h and stimulated by insulin (0.1 μM) for 30 min before lysed in 0.3% CHAPS buffer. The mTORC2 complex was purified by anti-HA beads. The immunoprecipitates were incubated with bacterially purified GST-Akt-tail in the presence of ATP and kinase buffer. The reactions were stopped by the addition of loading buffer. Akt-pS473 was examined by IB analysis.

I-K. Ectopically expressed Rb-WT (**I**) and Rb-13E (**J**), but not Rb-13A (**K**), compete with Sin1 in binding Akt1 in cells. IB analysis of WCL and anti-Flag IP derived from U2OS cells lysed in 0.3% CHAPS buffer 36 h after transfection with indicated constructs.

L. IB analysis of WCL and anti-Flag IP derived from U2OS cells lysed in 0.3% CHAPS buffer 36 h after transfection with the indicated constructs.

M. IB analysis of endogenous anti-Rb IP and WCL derived from $PTEN^{+/+}$ and $PTEN^{-/-}$ HCT116 cells lysed in 1% Triton buffer.

N. IB analysis of endogenous anti-Rb IP and WCL derived from MCF10A cells stably expressing PI3KCA oncogenic mutants (H1047R and E545K), with empty vector (EV) as a negative control.

(See also Figure S3)

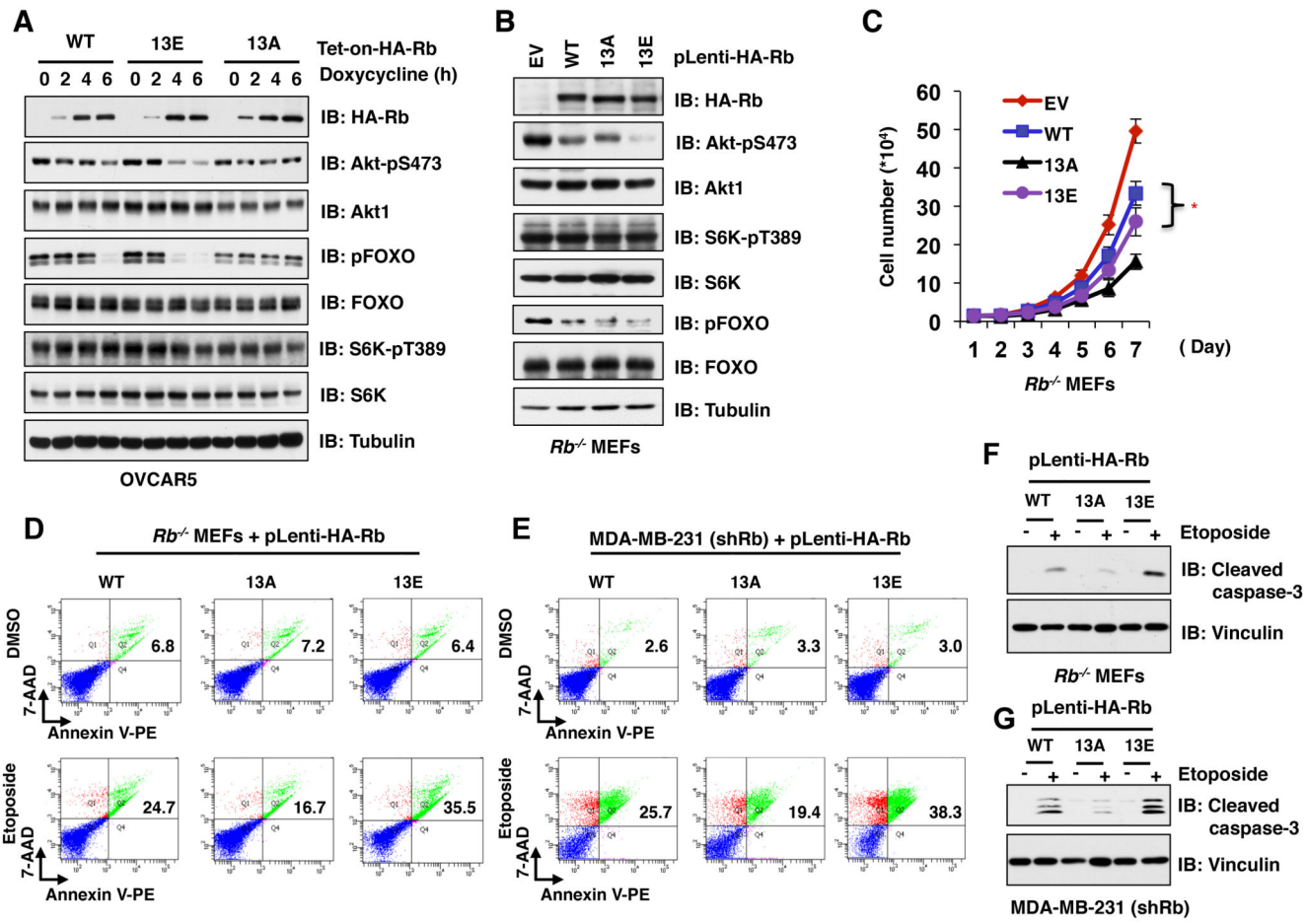

Figure 4. Hyper-phosphorylated Rb inhibits mTORC2 kinase activity to suppress cell proliferation and sensitize cells to chemotherapeutic treatment

A. IB analysis of WCL derived from OVCAR5 cells stably expressing inducible indicated HA-Rb constructs, which treated with 500 ng/ml doxycycline for the indicated periods.

B. IB analysis of WCL derived from *Rb*$^{-/-}$ MEFs stably expressing pLenti-hygro-EV, HA-Rb-WT, HA-Rb-13A and HA-Rb-13E.

C. Growth curve of *Rb*$^{-/-}$ MEFs stably expressing the indicated Rb constructs with empty vector (EV) as a negative control. Data are shown as mean ± s.d. from three independent experiments. * p<0.05 (t-test)

D. *Rb*$^{-/-}$ MEFs stably expressing the indicated Rb constructs were treated with 10 μM etoposide for 24 h before monitoring cell apoptosis by FACS.

E. *Rb*-depleted MDA-MB-231 cells stably expressing the indicated Rb constructs were treated with 20 μM etoposide for 48 h before monitoring cell apoptosis by FACS.

F. *Rb*$^{-/-}$ MEFs stably expressing the indicated Rb constructs were treated with 10 μM etoposide for 24 h before harvesting for IB analysis.

G. *Rb*-depleted MDA-MB-231 cells stably expressing the indicated Rb constructs were treated with 20 μM etoposide for 48 h before harvesting for IB analysis.

(See also Figure S4)

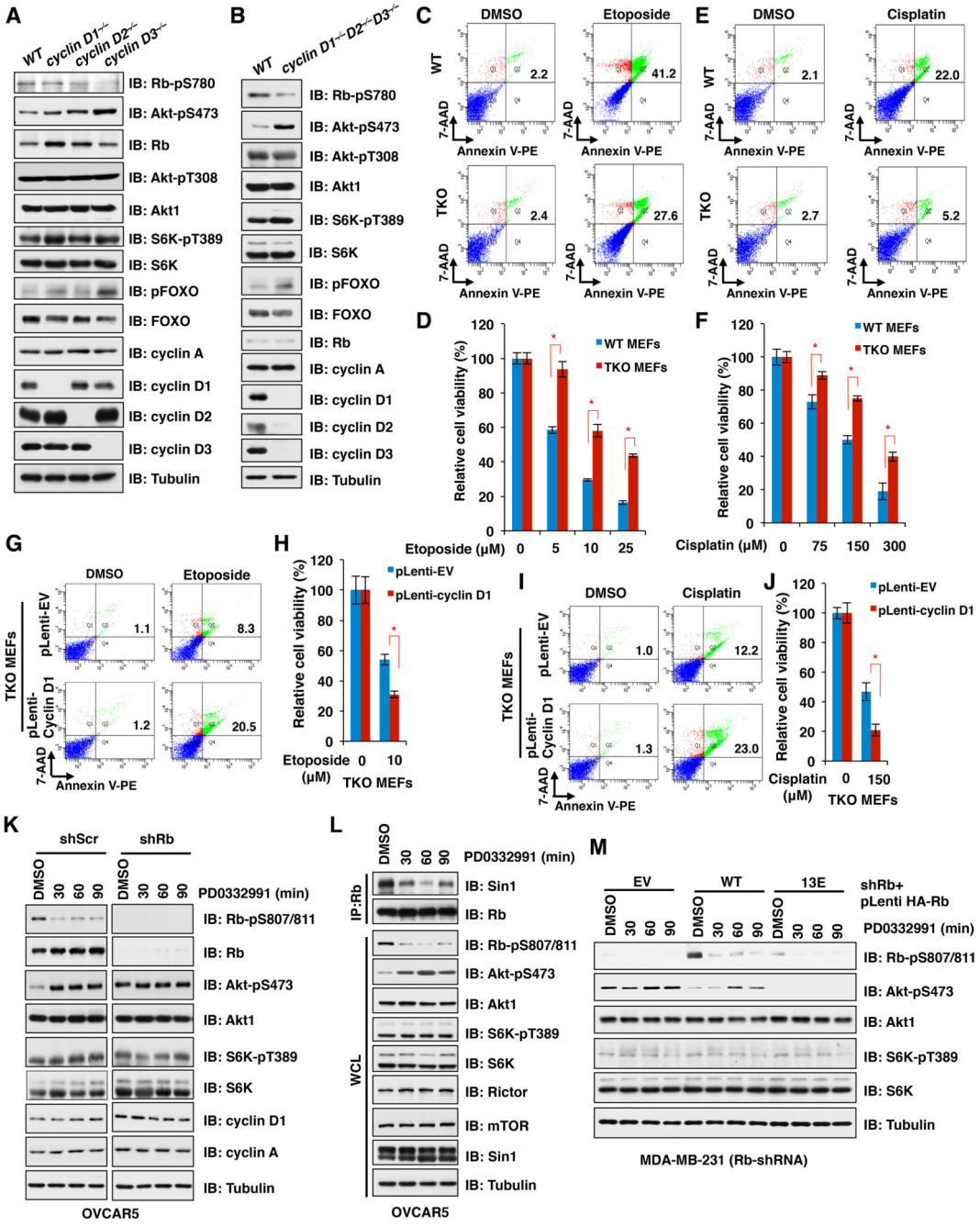

Figure 5. Inhibition of CDK4/cyclin D-mediated Rb phosphorylation by either genetic deletion of *cyclin D* or CDK4/6 inhibitor treatment leads to activation of mTORC2 to confer resistance to chemotherapeutic drugs

A. IB analysis of WCL derived from wild type MEFs, *cyclin D1*$^{-/-}$ MEFs, *cyclin D2*$^{-/-}$ MEFs and *cyclin D3*$^{-/-}$ MEFs.

B. IB analysis of WCL derived from wild type MEFs and *cyclin D1*$^{-/-}$*D2*$^{-/-}$*D3*$^{-/-}$ triple knockout (TKO) MEFs.

C and **E.** Wild type and TKO MEFs were treated with etoposide (10 μM) (**C**) or cisplatin (150 μM) (**E**) for 24 h. Cellular apoptosis was analyzed by flow cytometry.

D and **F.** Wild type and TKO MEFs were treated with indicated concentration of etoposide (**D**) or Cisplatin (**F**) for 24 h before performing cell viability assay. Data are shown as mean ± s.d. from three independent experiments. * $p<0.05$ (*t*-test)

G and **I.** TKO MEFs stable expression of cyclin D1 via lentiviral infection (with EV as a negative control) were treated with etoposide (10 μM) (**G**) or cisplatin (150 μM) (**I**) for 24 h before performing cell apoptosis assays.

H and **J.** TKO MEFs stably expressing cyclin D1 via lentiviral infection (with EV as a negative control) were treated with etoposide (10 μM) (**H**) or cisplatin (150 μM) (**J**) for 24 h before performing cell viability assay. Data are shown as mean ± s.d. from three independent experiments. * $p<0.05$ (*t*-test)

K. *Rb*-depleted OVCAR5 cells (with shScramble as a negative control) were treated with PD0332991 (500 nM) for the indicated time periods before harvesting for IB analysis.

L. IB analysis of WCL and endogenous Rb-immnuoprecipitates (IP) derived from OVCAR5 cells treated with PD0332991 (500 nM) for the indicated time periods.

M. *Rb*-depleted MDA-MB-231 cells stably expressing the indicated Rb constructs were treated with PD0332991 (500 nM) for the indicated time periods before harvesting for IB analysis.

(See also Figure S5)

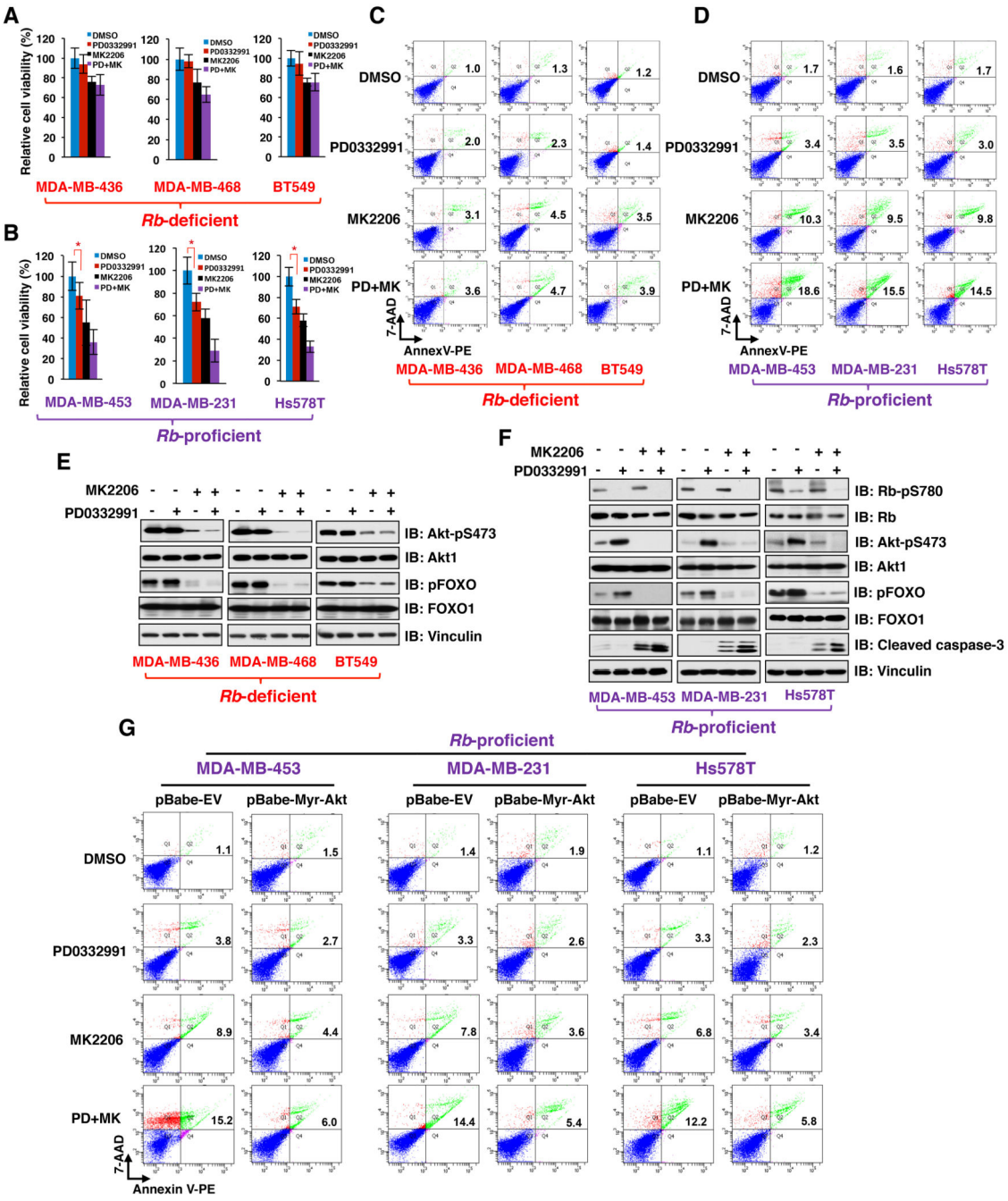

Figure 6. CDK4/6 inhibitor synergizes with the Akt inhibitor in treating *Rb*-proficient breast cancer cell lines

A and **B.** Human breast cancer cells with *Rb*-deficient (**A**) and proficient status (**B**) were treated with the CDK4/6 inhibitor PD0332991 (500 nM), or the Akt inhibitor MK2206 (1 μM), either alone or in combination for 48 h before performing cell viability assay. Data are shown as mean ± s.d. from three independent experiments. * $p<0.05$ (*t*-test)

C and **D.** Cell lines were treated with PD0332991 (500 nM), Akt inhibitor MK2206 (1 μM) or in combination for 48 h. Apoptosis was then monitored by flow cytometry. Data were

presented as both 7-AAD and Annexin V-PE staining. Cell populations were gated to illustrate the apoptotic cell population. Q1: dead cells; Q2: late apoptotic cells; Q3: non-apoptotic cells; Q4: early apoptotic cells.

E and **F.** Samples from **C** and **D** were also analyzed by IB analysis with the indicated antibodies.

G. *Rb*-proficient breast cancer cells stably expressing pBabe-EV or Myr-Akt were treated with CDK4/6 inhibitor PD0332991 (500 nM), or Akt inhibitor MK2206 (1 μM), either alone or in combination for 48 h before performing cell apoptosis assays by flow cytometry. (See also Figure S6)